Investigating the SO_2 absorption behavior of pyrimidine-based deep eutectic solvents *via* dual-site thermodynamic model

Yiru Zou,[ac] Xiaoxiao Xing,[a] Chao Wang,[c] Duanjian Tao,[*d] Haiyan Ji,[c] Peiwen Wu,[*c] Yanhong Chao,[a] and Wenshuai Zhu[*abc]

[a] College of Chemical Engineering and Environment, State Key Laboratory of Heavy Oil Processing, College of Science, China University of Petroleum-Beijing, Beijing 102249, PR China, E-mail address: zhuws@cup.edu.cn

[b] Shandong Key Laboratory of Green Electricity & Hydrogen Science and Technology, Shandong Institute of Petroleum and Chemical Technology, Dongying 257061, PR China

[c] School of Chemistry and Chemical Engineering, School of the Environment and Safety Engineering, School of Materials Science and Engineering, Jiangsu University, Zhenjiang 212013, PR China

[d] College of Chemistry and Chemical Engineering, Jiangxi Normal University, Nanchang 330022, PR China

1. Gas Absorption:

Using a "double-tank" gas absorption device, the absorption experiment of SO_2 or CO_2 was carried out. As shown in **Scheme S1**, the volume of the gas storage tank (GT) is 122.300 cm^3, denoted as V_{GT}; The volume of the absorption tank (AT) is 46.187 cm^3, and it is equipped with a magnetic stirrer with a certain volume, denoted as V_{AT}. A magnetic stirrer (MS) is equipped directly below the absorption tank, and its rotation speed is kept at 350 rpm. The pressure sensors PV and SV are used to measure the pressure of the gas storage tank and absorption tank and transmit it to the computer (CP), denoted as *P1i GT* and *P2i AT* (i = 0, 1, 2, 3, ..., *n*). The measurement accuracy of the temperature control device in the constant temperature water bath (CT) is ± 0.1 K, which is used to adjust the temperature of the absorption tank and the gas storage tank, so as to explore the gas absorption performance at different temperatures. The vacuum pump (VP) is used to evacuate the air or N_2 in the tank before gas absorption,

and to remove the remaining acid gas in the tank after absorption. To protect personnel safety and prevent harmful gases from being directly discharged into the atmosphere, the remaining acid gases should be slowly introduced into high-concentration sodium hydroxide (NaOH) solution for tail gas treatment.

In a typical absorption experiment, a certain mass of sample (w) was weight with an analytical balance (with an accuracy of ± 0.0001 g) and put it into an absorption tank. After sealing the device, put it in a constant temperature water bath, and set the required temperature (298.15 K, 313.15 K, 333.15 K and 353.15 K). After the temperature of each part stabilizes, turn off F1 and F2, then turn on F3, F4, and VP to empty the gas storage tank and absorption tank. After the pressure stabilizes, turn off F3, F4, and VP. At this time, the indication of PV is *P10 GT*, and the indication of SV is *P20 AT*. Pour a certain amount of SO_2 or CO_2 into the gas storage tank and close F_1. After the PV display is stable, it is recorded as *P11 GT*, and the SV display is recorded as *P21 AT*. At this time, the pressure of SO_2 or CO_2 in the gas storage tank is $P_{GT1} = P11\ GT - P10\ GT$. Turn on the magnetic stirrer, slowly introduce a certain amount of SO_2 or CO_2 into the suction tank, and then close F_3. After the number of SV is stable, it is recorded as *P2i AT* (i = 2, 3, 4, ..., *N*), The pressure of SO_2 or CO_2 in the absorption tank is recorded as $P_{ATi} = P2i\ AT - P21\ AT$. At this time, the indication of PV is recorded as *P1i GT* (i = 2, 3, 4, ..., *N*), and the pressure of SO_2 or CO_2 in the gas tank is recorded as $P_{GTi} = P2i\ GT - P20\ GT$. Then, the absorption capacity (m_{gas}) of SO_2 or CO_2 gas is calculated by eq (S1):

$$m_{gas}\ (g/g) = [\rho PGT1\ gas \cdot V_{GT} - \rho PGTi\ gas \cdot V_{GT} - \rho PATi\ gas\ (V_{AT} - w/\rho)]/w \quad (S1)$$

Where $\rho PGT1\ gas$, $\rho PGTi\ gas$, and $\rho PATi\ gas$ represent the gas density (g cm^{-3}) of P_{GT1}, P_{GTi} and P_{ATi}, respectively, and the values are obtained from the NIST Chemistry WebBook database; V_{GT} and V_{AT} represent the volume (cm^3) of the gas storage tank and the absorption tank, respectively; w and ρ represent the mass (g) and density (g cm^{-3}) of the DESs, respectively.

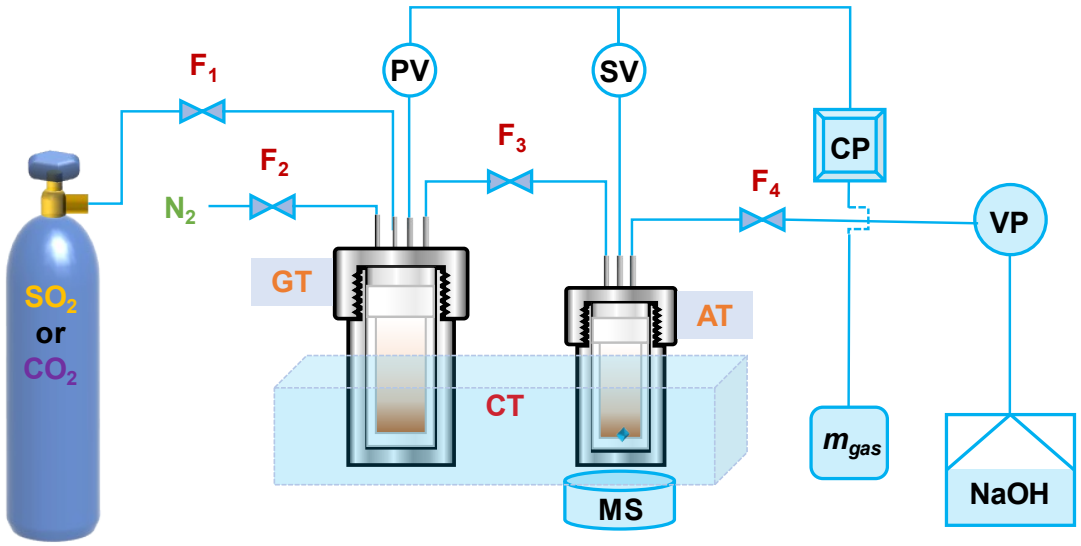

Scheme S1. Schematic diagram of gas absorption device (GT: gas storage tank; AT: absorption tank; CT: constant temperature water bath; MS: magnetic stirrer; F_1 ~ F_4: gas valves; PV, SV: pressure sensors; CP: computer; VP: vacuum pump)

Absorption-desorption Experiment: The regeneration performance of DESs was investigated, and the specific operations were as follows: First, under the conditions of 298.15 K and 1.0 bar, the SO_2 absorption experiment was carried out. Then, the vacuum pump and F_3, F_4 were turn on to remove the residual gas, and raise the temperature to 353.15 K. Continue to evacuate for 60 min, open F_2 and introduce N_2 to exhaust SO_2; Turn off F_2 and reduce the temperature to 298.15K. After the temperature is stable, close F_3, F_4 and vacuum pump, and carry out the absorption experiment.

2. Materials and Characterizations:

***Materials*:** Sulfur dioxide (SO_2, 99.99%) was obtained from Nanjing Hongye Special Gas Supply Co., Ltd. Carbon dioxide (CO_2, 99.99%) was obtained from Zhenjiang Zhongpu Gas Company. 2-Aminopyrimidine (AmPyr, 98%), 2-Chloropyrimidine (ChPyr, 99%), 2-Bromopyrimidine (BrPyr, 98%), 4-Amino-2-hydroxypyrimidine (Cyt, 98%), 2,4-Dihydroxypyrimidine (Ura, 99%), 3-Aminopyridazine (AmPd, 98%), 2-Aminopyrazine (AmPz, 99%) and 2,4,6-Triaminopyrimidine (TAmPyr, 98%) were purchased from Aladdin Reagent (Shanghai) Co., Ltd. 4,6-Diaminopyrimidene (DAmPyr, 98%) was purchased from

Shanghai Macklin Biochemical Co., Ltd. Dimethylsulfoxide-d6 (DMSO-d_6, 99.9%) was purchased from Shanghai Macklin Biochemical Co., Ltd. 1-ethyl-3-methylimidazolium Chloride (C_2mimCl, 99%) and 1-ethyl-3-methylimidazolium Bromide (C_2mimBr, 99%) were purchased from Shanghai Chengjie Chemical.

Characterizations: The density of as-prepared DESs were measured from 293.15 - 353.15 K *via* Anton Paar densimeter (DMA 4500m) with an uncertainty of 0.00001 g cm^{-3}. The viscosity was measured by HR-103060000 with 5% uncertainty over a measurement range of 273.15 - 353.15 K. Under N_2 atmosphere, thermogravimetric analysis (TGA) was performed using a STA449C Jupiter Simultaneous Thermal Analyzer and heated from room temperature to 800 K at a heating rate of 10 K min^{-1}. The mechanism of SO_2 absorption was investigated *via* FT-IR and ^{1}H-NMR. The FT-IR measurement of the sample used an Attenuated Total Reflection (ATR) detector, which does not require the addition of KBr for tablet pressing and can directly analyze solids, liquids, films, *etc*. After ensuring the ATR crystal surface was clean and uncontaminated, a background signal was scanned with an empty light path without placing any sample. For liquid samples, 1-2 drops were added to the center circle of the ATR crystal using a dropper or syringe (for solid samples, an appropriate amount sufficed). The sample spectrum was scanned after confirming the sample completely covered the crystal. The ^{1}H-NMR was measured using DMSO-d_6 as a solvent (Bruker Avance 400 MHz spectrometer).

Table S1 Densities (g cm^{-3}) of C_2mimCl-*n* + AmPyr (*n* = 2, 3, 4, 5, 6, 7).

Entry	293.15 K	298.15 K	303.15 K	308.15 K	313.15 K	323.15 K	333.15 K	343.15 K	353.15 K
2	1.1675	1.1644	1.1614	1.1584	1.1554	1.1493	1.1433	1.1372	1.1312
3	1.1619	1.1589	1.1559	1.1530	1.1500	1.1441	1.1382	1.1323	1.1264
4	1.1585	1.1556	1.1526	1.1497	1.1468	1.1409	1.1351	1.1292	1.1235
5	1.1562	1.1532	1.1503	1.1474	1.1445	1.1386	1.1328	1.1270	1.1214
6	1.1547	1.1518	1.1489	1.1460	1.1431	1.1373	1.1316	1.1258	1.1202
7	1.1537	1.1507	1.1478	1.1450	1.1421	1.1363	1.1306	1.1249	1.1192

Table S2 Density (g cm^{-3}) of C_2mimCl-7 + HBDs.

Entry	293.15 K	298.15 K	303.15 K	308.15 K	313.15 K	323.15 K	333.15 K	343.15 K	353.15 K
BrPyr	1.1988	1.1956	1.1925	1.1894	1.1863	1.1801	1.1740	1.1681	1.1622
Ura	1.1690	1.1661	1.1632	1.1603	1.1574	1.1516	1.1460	1.1403	1.1347
Cyt	1.1676	1.1647	1.1619	1.1591	1.1562	1.1506	1.1451	1.1395	1.1340
DAmPyr	1.1650	1.1621	1.1593	1.1564	1.1536	1.1479	1.1423	1.1367	1.1311
ChPyr	1.1635	1.1605	1.1575	1.1545	1.1516	1.1457	1.1399	1.1341	1.1284
AmPyr	1.1537	1.1507	1.1478	1.1450	1.1421	1.1363	1.1306	1.1249	1.1192
AmPd	1.1534	1.1505	1.1476	1.1448	1.1419	1.1362	1.1305	1.1249	1.1195
AmPz	1.1513	1.1484	1.1456	1.1427	1.1398	1.1342	1.1286	1.1230	1.1175

Table S3 Density fitting parameters of C_2mimCl-*n* + AmPyr (*n* = 2, 3, 4, 5, 6, 7).

Parameters	2	3	4	5	6	7
α_1 (g cm^{-3})	1.3447	1.3352	1.3298	1.3264	1.3235	1.3219
$\beta_1 \times 10^{-4}$ (g cm^{-3} K)	-6.0467	-5.9118	-5.8427	-5.8099	-5.7590	-5.7416
R2 1	0.9999	0.9999	0.9998	0.9996	0.9998	0.9998

Table S4 Density fitting parameters of C_2mimCl-7 + HBDs.

Parameters	HBDs							
	BrPyr	Ura	Cyt	DAmPyr	ChPyr	AmPyr	AmPd	AmPz
α_2 (g cm^{-3})	1.3776	1.3366	1.3316	1.3305	1.3349	1.3219	1.3194	1.3164
$\beta_2 \times 10^{-4}$ (g cm^{-3} K)	-6.1056	-5.7210	-5.5971	-5.6475	-5.8509	-5.7416	-5.6651	-5.6360
R2 2	0.9998	0.9999	0.9999	0.9999	0.9999	0.9999	0.9999	0.9999

Table S5 Viscosity (Pa s) of C_2mimCl-*n* + AmPyr (*n* = 2, 3, 4, 5, 6, 7).

Entry	293.15 K	298.15 K	303.15 K	313.15 K	323.15 K	333.15 K	343.15 K	353.15 K
2	4.0670	2.2807	1.3169	0.5433	0.2689	0.1513	0.1007	0.0794
3	3.3194	1.8788	1.0973	0.4665	0.2367	0.1455	0.1035	0.0812
4	3.1815	1.8450	1.0962	0.4795	0.2487	0.1437	0.0925	0.0675
5	2.9871	1.7520	1.0531	0.4623	0.2412	0.1432	0.0976	0.0849
6	2.5186	1.5188	0.9298	0.3996	0.2171	0.1339	0.0920	0.0798
7	2.3447	1.3884	0.8467	0.3855	0.2066	0.1224	0.0829	0.0653

Table S6 Viscosity (Pa s) of HBAs-7 + HBDs.

Entry	293.15 K	298.15 K	303.15 K	313.15 K	323.15 K	333.15 K	343.15 K	353.15 K
a	2.5680	1.6355	1.0510	0.5331	0.2901	0.1768	0.1180	0.0918
b	2.3447	1.3884	0.8467	0.3855	0.2066	0.1224	0.0829	0.0653
c	2.2717	1.4804	0.9785	0.5014	0.2758	0.1701	0.1117	0.0906
d	1.9499	1.2093	0.7729	0.3755	0.2096	0.1239	0.0891	0.0799
e	1.2998	0.8594	0.5805	0.3116	0.1803	0.1182	0.0857	0.0736
f	0.8651	0.5771	0.3969	0.2156	0.1324	0.0885	0.0636	0.0544
g	0.6081	0.4247	0.3013	0.1739	0.1085	0.0754	0.0545	0.0450
h	0.5059	0.3688	0.2742	0.1613	0.1001	0.0725	0.0607	0.0505
i	0.3018	0.2256	0.1686	0.1063	0.0719	0.0531	0.0418	0.0349

a: C_2mimCl-7 + Cyt; *b*: C_2mimCl-7 + AmPyr; *c*: C_2mimCl-7 + DAmPyr; *d*: C_2mimCl-7 + AmPd; *e*: C_2mimCl-7 + Ura; *f*: C_2mimCl-7 + AmPz; *g*: C_2mimCl-7 + ChPyr; *h*: C_2mimBr-7 + AmPyr; *i*: C_2mimCl-7 + BrPyr.

Table S7 Viscosity fitting parameters of C_2mimCl-*n* + AmPyr (*n* = 2, 3, 4, 5, 6, 7).

Parameters	2	3	4	5	6	7
$\eta_0 \times 10^4$ (Pa s)	2.546 ± 1.550	6.194 ± 3.545	3.625 ± 1.770	4.804 ± 2.894	3.109 ± 2.828	5.847 ± 2.319
t_1 (K)	744.9 ± 95.64	589.1 ± 81.05	694.45 ± 77.03	653.3 ± 93.383	728.3 ± 152.8	601.2 ± 59.98
T_0 (K)	216.2 ± 4.886	224.6 ± 4.675	216.7 ± 4.241	218.4 ± 5.363	212.3 ± 8.588	220.7 ± 3.644
R2 3	0.999	0.999	0.999	0.999	0.999	0.999

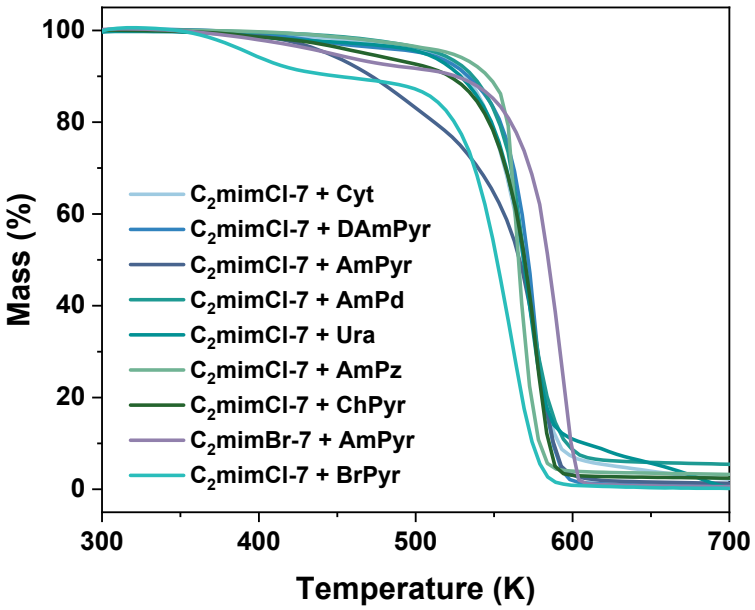

Fig. S1 TG analysis diagrams of pyrimidine-based DESs.

Table S8 the comparison of SO_2 absorption with other materials.

Absorbents	Temperature (K)	Pressure (bar)	m_{SO2} (mol kg^{-1})[a]	Reference
NiBDP	298	1.0	8.48	S1
Mg_2(dobpdc)	298	1.0	19.5	S2
HIAM-330	298	1.0	12.1	S3
SIFSIX-7-Cu	298	1.0	14.7	S4
Zr-bptc	298	1.0	7.8	S5
MFM-133	298	1.0	8.9	S5
MFM-422	298	1.0	13.6	S5
DUT-8	293	0.97	13.99	S6
DMOF	293	0.97	13.09	S6
DMOF-NDC	293	0.97	10.09	S6
DMOF-ADC	293	0.97	6.51	S6
NU-1801(Y)	298	1.0	8.78	S7
NU-1801(Zr)	298	1.0	10.98	S7
NU-1801(Hf)	298	1.0	8.45	S7
NU-1801(Ce)	298	1.0	8.59	S7
NU-1801(Th)	298	1.0	5.31	S7
6FT-RCC3	298	1.0	13.78	S8
MOC-Pd-BF_4	298	1.0	3.63	S9
MOC-Pd-NO_3	298	1.0	5.98	S9
C_2mimBr-7 + AmPyr	298	1.0	14.630	This work
C_2mimCl-7 + BrPyr	298	1.0	17.704	This work
C_2mimCl-7 + Ura	298	1.0	17.791	This work
C_2mimCl-7 + AmPz	298	1.0	18.017	This work
C_2mimCl-7 + ChPyr	298	1.0	18.062	This work
C_2mimCl-7 + Cyt	298	1.0	18.243	This work
C_2mimCl-7 + DAmPyr	298	1.0	18.595	This work
C_2mimCl-7 + AmPd	298	1.0	18.746	This work
C_2mimCl-7 + AmPyr	298	1.0	19.032	This work

[a] The units of mol kg^{-1} and mmol g^{-1} are the same.

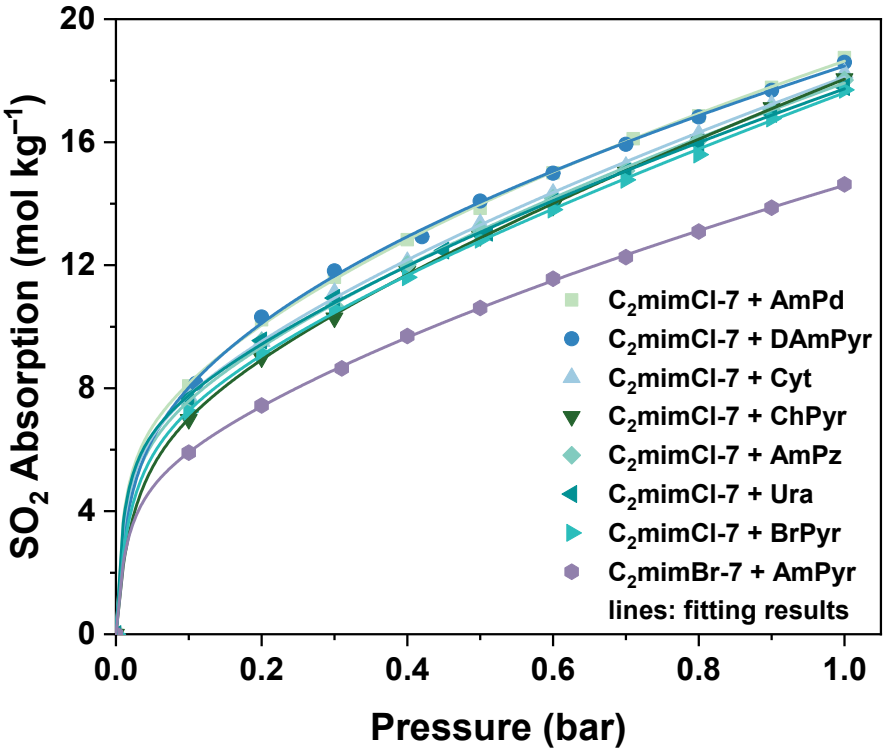

Fig. S2 DS-DETM equation fitting of pyrimidine-based DESs for SO_2 absorption at 298.15K.

Table S9 Calculated Henry's constants, reaction equilibrium constants, and *R2 6* of SO_2 absorption in pyrimidine-based DESs.

Parameters	*H* (bar)	k_{HBAs}	k_{HBDs}	*R2 6*
C_2mimCl-7 + AmPd	0.17924	105.83109	1.49431	0.999
C_2mimCl-7 + DAmPyr	0.17705	64.47111	2.06037	0.999
C_2mimCl-7 + Cyt	0.15649	89.83788	1.23746	0.999
C_2mimCl-7 + ChPyr	0.13961	43.40060	0.93549	0.999
C_2mimCl-7 + AmPz	0.1689	76.12600	1.00501	0.999
C_2mimCl-7 + Ura	0.16222	102.09880	1.17318	0.999
C_2mimCl-7 + BrPyr	0.13774	55.89346	1.37954	0.999
C_2mimBr-7 + AmPyr	0.22827	70.53194	0.92582	0.999

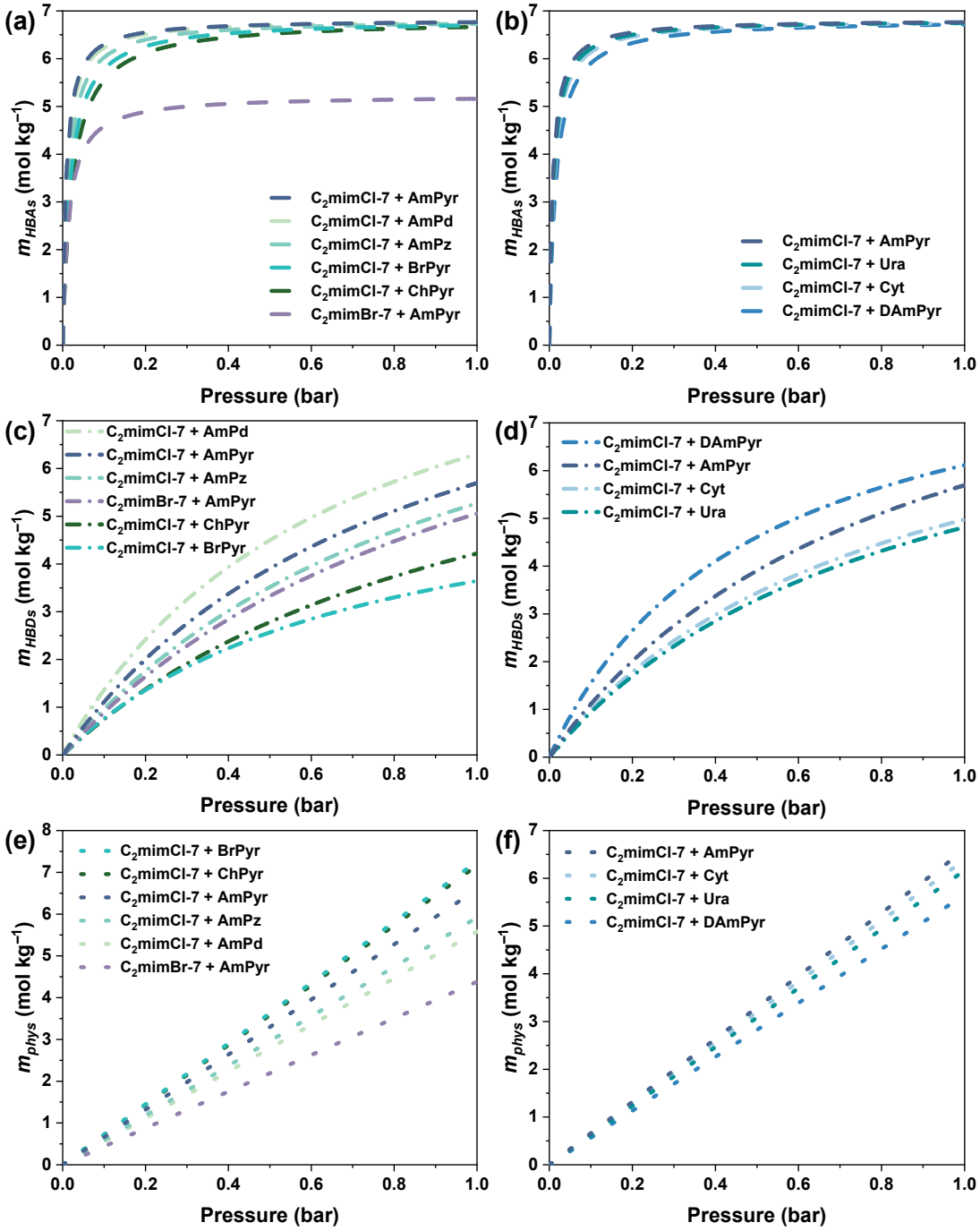

Fig. S3 The calculated m_{phys}, m_{HBAs}, and m_{HBDs} of corresponding HBAs-7 + HBDs DESs at 298.15 K; Comparison between C_2mimCl-7 + AmPyr and (a, c, e) monofunctional or (b, d, f) multifunctional DESs.

Table S10 The SO_2 absorption capacity and selectivity of the DESs compare with other absorbents.

Absorbents	Temperature (K)	m_{SO2} (mol kg^{-1})	Selectivity (SO_2/CO_2)	Reference
DMI	293.15	14.332	—	S10
DMPU	293.15	13.620	—	S10
TMU	293.15	14.054	—	S10
[emim]Cl+DCDA (3:1)	298.15	16.58	—	S11
PEG 200-EmimCl (1:1)	298.2	10.95	12.8	S12
TeEG-EminCl (1:1)	298.2	12.48	14.2	S12
TeEG-EmimCl (1:2)	298.2	13.25	29.9	S12
[TMEA][MOAc]	303.2	10.424	86.83	S13
[EimH]Cl/EG (1:2)	293.2	8.366	—	S14
[EimH]Cl/EG (1:1)	293.2	9.814	—	S14
[EimH]Cl/EG (2:1)	293.2	11.10	—	S14
[EimH]Cl/EG (3:1)	293.2	11.60	655	S14
EmimCl + 6-HoP-7	298.15	17.213	491.8	S15
EmimCl + 6-AmP-7	298.15	18.118	517.7	S15
EmimCl + 6-ChP-7	298.15	17.399	527.2	S15
C_2mimCl-7 + ChPyr	298.15	18.062	451.6	This work
C_2mimCl-7 + Ura	298.15	17.791	494.2	This work
C_2mimCl-7 + AmPyr	298.15	19.032	528.7	This work
C_2mimCl-7 + BrPyr	298.15	17.704	536.5	This work
C_2mimCl-7 + DAmPyr	298.15	18.595	808.5	This work
C_2mimCl-7 + Cyt	298.15	18.243	1073.1	This work

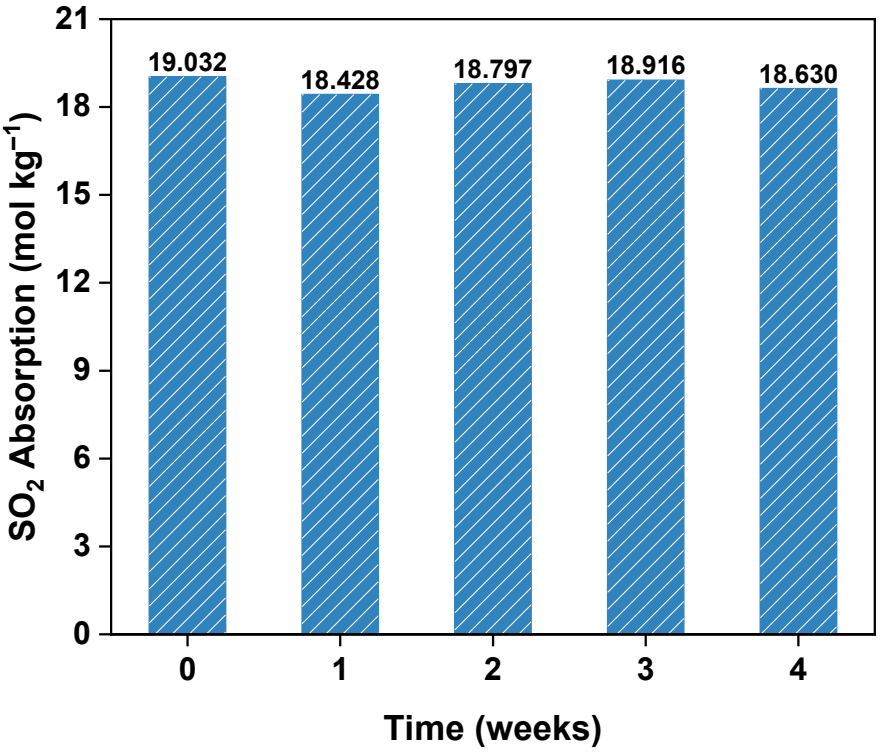

Fig. S4 The stability of C_2mimCl-7 + AmPyr; T = 298.15 K, P = 1.0 bar.

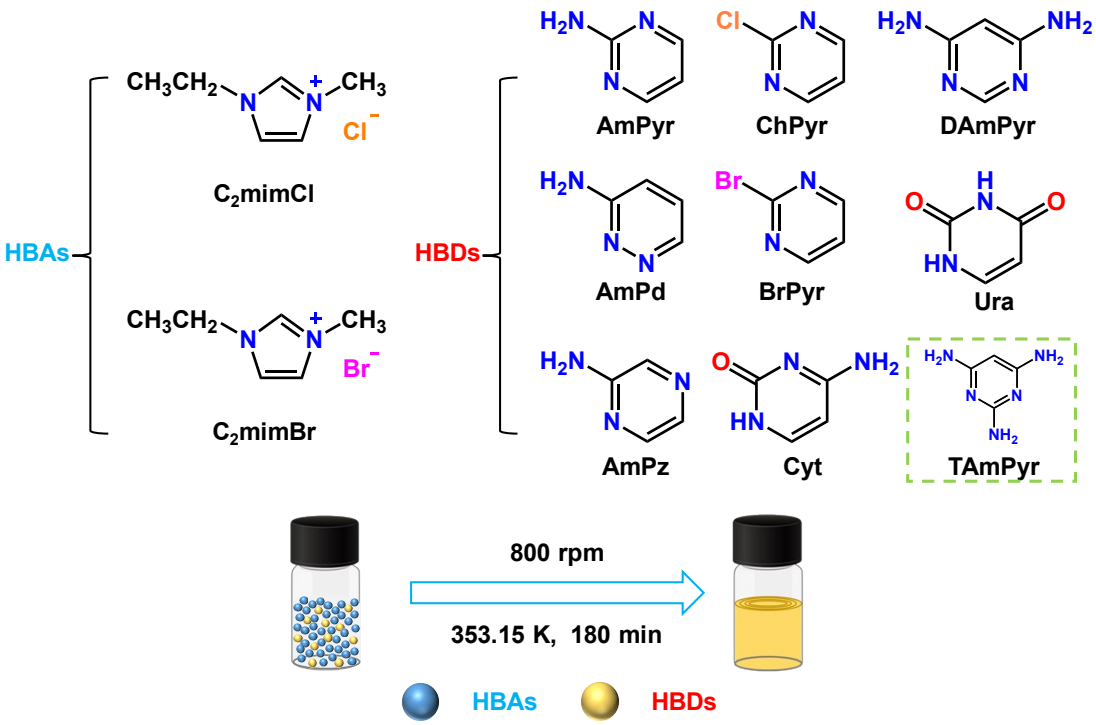

Scheme S2 The structural formulas of HBAs and HBDs, as well as the preparation process of DESs.

References

S1 J.L. Obeso, K. Gopalsamy, M. Wahiduzzaman, E. Martínez-Ahumada, D. Fan, H.A. Lara-García, F.J. Carmona, G. Maurin, I.A. Ibarra and J.A.R. Navarro, Impact of Ni(ii) coordinatively unsaturated sites and coordinated water molecules on SO_2 adsorption by a MOF with octanuclear metal clusters, *J. Mater. Chem. A*, 2024, **12**, 10157-10165.

S2 E. Martínez-Ahumada, D.w. Kim, M. Wahiduzzaman, P. Carmona-Monroy, A. López-Olvera, D.R. Williams, V. Martis, H.A. Lara-García, S. López-Morales, D. Solis-Ibarra, G. Maurin, I.A. Ibarra and C.S. Hong, Capture and detection of SO_2 using a chemically stable Mg(ii)–MOF, *J. Mater. Chem. A*, 2022, **10**, 18636-18643.

S3 L. Yu, M. He, J. Yao, Q. Xia, S. Yang, J. Li and H. Wang, A robust aluminum-octacarboxylate framework with scu topology for selective capture of sulfur dioxide, *Chem. Sci.*, 2024, **15**, 8530-8535.

S4 J. Ren, W. Zeng, Y. Ying, D. Liu and Q. Yang, Discovery of anion-pillared metal–organic frameworks for efficient SO_2/CO_2 separation via computational screening, *AIChE J.*, 2024, **70**, e18351.

S5 J. Li, G.L. Smith, Y. Chen, Y. Ma, M. Kippax-Jones, M. Fan, W. Lu, M.D. Frogley, G. Cinque, S.J. Day, S.P. Thompson, Y. Cheng, L.L. Daemen, A.J. Ramirez-Cuesta, M. Schröder and S. Yang, Structural and dynamic analysis of sulphur dioxide adsorption in a series of zirconium-based metal–organic frameworks, *Angew. Chem. Int. Edit.*, 2022, **61**, e202207259.

S6 S. Xing, A. Mohabbat, I. Boldog, J. Möllmer, M. Lange, Y. Haiduk, T. Heinen, V. Pankov, O. Weingart and C. Janiak, Rational fine-tuning of mof pore metrics: Enhanced SO_2 capture and sensing with optimal multi-site interactions, *Adv. Funct. Mater.*, 2025, 2503013.

S7 C. Zhang, Y. Xie, H. Xie, X. Wang, F. Sha, K.O. Kirlikovali, X. Wang, Y. Chen, G.W. Peterson and O.K. Farha, Interrogating the metal identity effect of isostructural NU-1801 frameworks on toxic gas capture with moisture-enhanced feature, *ACS Appl. Mater. Interfaces*, 2025, **17**, 64910-64920.

S8 E. Martínez-Ahumada, D. He, V. Berryman, A. López-Olvera, M. Hernandez, V. Jancik, V. Martis, M.A. Vera, E. Lima, D.J. Parker, A.I. Cooper, I.A. Ibarra and M. Liu, SO_2 capture using porous organic cages, *Angew. Chem. Int. Edit.*, 2021, **60**, 17556-17563.

S9 E.G. Percástegui, E. Sánchez-González, S. de Jesús Valencia-Loza, S. Cruz-Nava, V. Jancik and D. Martínez-Otero, Counterions determine if metal-organic cages convert SO_2 to sulfate or reversibly adsorb it, *Angew. Chem. Int. Edit.*, 2024, e202421169

S10 Y. Jiang, X. Liu and D. Deng, Solubility and thermodynamic properties of SO_2 in three low volatile urea derivatives, *J. Chem. Thermodyn.*, 2016, **101**, 12-18.

S11 X. Wu, R. Guan, W. Zheng and K. Huang, New deep eutectic solvents formed by 1-ethyl-3-methylimidazolium chloride and dicyandiamide: Physiochemical properties and SO_2 absorption performance, *J. Taiwan Inst. Chem. E.*, 2021, **119**, 45-51.

S12 M. Liu, T. Zhao, H. Dong, Y. Xu and C. Zhu, Absorption of SO_2 by deep eutectic solvents composed of EmimCl and dihydric alcohols: Thermodynamic and absorption mechanism studies, *J. Mol. Liq.*, 2023, **369**, 120878.

S13 P. Liu, K. Cai, X. Zhang, X. Wang, M. Xu, F. Liu and T. Zhao, Rich ether-based protic ionic liquids with low viscosity for selective absorption of SO_2 through multisite interaction, *Ind. Eng. Chem. Res.*, 2022, **61**, 5971-5983.

S14 P. Zhang, Z. Tu, X. Zhang, X. Hu and Y. Wu, Acidic protic ionic liquid-based deep eutectic solvents capturing SO_2 with low enthalpy changes, *AIChE J.*, 2023, **69**, e18145.

S15 Y. Zou, C. Wang, H. Ji, P. Wu, Y. Chao, X. Yu, Z. Yu, H. Liu, Z. Liu and W. Zhu, Rapid, selectivity, and reversibility absorption of SO_2 via purine-based deep eutectic solvents and thermodynamic analysis, *Green Chem. Eng.*, 2024, DOI: 10.1016/j.gce.2024.1010.1005.